AN APPROACH TO THE MODELLING OF A VIRTUAL THERMAL MANIKIN

by

Dragan A. RUŽIĆ [a]* and Siniša M. BIKIĆ [b]

[a] Department for Mechanization and Design Engineering, Faculty of Technical Sciences, University of Novi Sad, Novi Sad, Serbia
[b] Department for Energy and Process Engineering, Faculty of Technical Sciences, University of Novi Sad, Novi Sad, Serbia

Original scientific paper
DOI: 10.2298/TSCI130115115R

The aim of the research described in this paper, is to make a virtual thermal manikin that would be simple, but also robust and reliable. The virtual thermal manikin was made in order to investigate thermal conditions inside vehicle cabins. The main parameters of the presented numerical model that were investigated in this paper are mesh characteristics and turbulence models. Heat fluxes on the manikin's body segments obtained from the simulations were compared with published results, from three different experiments done on physical thermal manikins. The presented virtual thermal manikin, meshed with surface elements of 0.035 m in nominal size (around 13,600 surface elements) and in conjunction with the two-layer RANS Realizable k-ε turbulence model, had generally good agreement with experimental data in both forced and natural flow conditions.

Key words: *virtual thermal manikin, computational fluid dynamics, dry heat loss, vehicle cabin*

Introduction

An evaluation of thermal conditions in a vehicle cabin can be done in one of the following three ways: by using human subjects, by direct measurement of microclimate physical quantities or by using special human-shaped sensors, the so called thermal manikins. The first thermal manikins were developed in the 1940s for military research purposes. In automotive application, thermal manikins appeared in the 1980s, and they have been in constant development ever since [1, 2]. Apart from experimental methods, numerical methods for research of vehicle cabin microclimate are also used. These are usually computational fluid dynamic (CFD) techniques. In both experimental and numerical methods, thermal conditions must be related to the thermal sensations of the driver and of the passengers. For this purpose, various thermal sensation indices are introduced, for example equivalent temperature. Equivalent temperature is defined as the temperature of a homogenous space, with mean radiant temperature equal to air temperature and zero air velocity, in which a person has the same heat loss by convection and radiation as in the actual conditions. The equivalent temperature can be determined using thermal manikins, according to the ISO 14505-2 standard [3].

* Corresponding author; e-mail: ruzic@uns.ac.rs

In a numerical investigation of thermal conditions in a cabin, some kind of a virtual human body needs to be used. A model of the human body that is geometrically and thermally appropriate is called a computer simulated person (CSP), like those described in [4, 6, 8, 9]. Han *et al.* [4] used the Berkeley Thermal Comfort Model (BTCM) in the development of Virtual Thermal Comfort Engineering, a technique intended for the simulation of automotive passenger compartment climatic conditions. This model was based on Stolwijk's model of human thermoregulation and it was capable of predicting physiological response in transient and/or non-uniform environment, for example in motor vehicles [5]. Voelker and Kornadt [6] also coupled the BTCM with a virtual human body to investigate human microclimate conditions using STAR-CCM+ software. Their virtual model of the body is a 3-D laser scan of a real thermal manikin called *Feelix*, and it is divided into 16 segments. Tanabe *et al.* [7] developed a virtual human body model that had a 65-node model of the thermoregulation (65MN). The body was divided into 16 segments, each of which consisted of four layers plus blood. The male human body model with 4,369 surface elements was used for radiation analysis, while a simplified model with 1,542 surfaces was used for CFD simulations. The thermal sensation was evaluated from skin temperature, skin wetness and the total heat loss from the virtual manikin's surface. The virtual model of the human body described in Kilic and Sevilgen [8] had simplified physiological shape modelled in CAD software, with no clothes. The manikin surface was divided into 17 segments. The thermo-physiological model was based on Gagge's two-node model, and the simulation results were validated with experimental and theoretical data. The model introduced by Zhu *et al*. [9] was derived from the coupling of his seated human body model with Sakoi's human thermal physiological model. The body model divided into 16 segments was made of 6,050 triangular elements. This 3-D physiological model had all internal body parts and blood flow. The latent heat transfer over the body was based on the sweat rate, which was calculated according to the Fanger's model. As can be noted from results given in [9], a complex model of the human body thermoregulation system does not guarantee the absence of discrepancies between experimental and numerical results.

When the geometric shape and/or thermoregulation of the CSP are simplified, it is more appropriate to call this model a virtual thermal manikin (VTM). The models that were considered in the development of the VTM described in this paper are those based on dry heat exchange [2, 10, 11]. Nilsson [2] introduced a virtual manikin called “MANIKIN3”, which was in a simplified humanoid shape and divided into 18 zones. Its surface temperature was calculated iteratively, in relation to segment clothing insulation and total dry heat flux. This manikin was made to be used for equivalent temperature prediction in Fluent, CFX or STAR-CD software. Sorensen and Voigt [10] modelled a seated female person based on the real manikin manufactured by Teknik, Denmark. The STAR-CD virtual model had 23,000 surface elements and the domain was divided into more than one million elements. The manikin's body was divided into 16 segments with the surface temperature set to 31 °C. Under the conditions of natural convection flow, the heat fluxes and the local air velocities predicted from the CFD showed good agreement with the experimental data from de Dear *et al*. [12], as well as with the measurements done by PIV (Particle Image Velocimetry) on the thermal manikin made by Teknik. In the study of Martinho *et al.* [11], the virtual manikin, virtual chamber, and boundary conditions were made according to the benchmark tests by Nilsson *et al.* [13, 14]. The ANSYS-CFX virtual manikin had 95,062 surface elements, while the domain was divided into more than 1.4 million elements. In their study, boundary conditions, turbulence models and mesh size were analyzed in terms of accuracy of the simulation results in comparison with experimental results. They concluded that

physical approximation errors, the turbulence modeling and near wall treatment, as well as the number of mesh elements, can lead to significant differences in CFD results and, consequently, between predicted and experimental results.

For clarification purposes, the term VTM will be used only to denote the virtual thermal manikin being described in this paper. The VTM presented in this paper is to be used in the comparative evaluation and the optimization of the vehicle ventilation system, using the equivalent temperature as a criterion. An example of the use of the VTM in an agricultural tractor cab is given in [15]. Since there are many different combinations of boundary conditions and air-conditioning system settings, it is necessary to perform a large number of virtual experiments. Therefore, in order to reduce computational time, the model has to be simple but sufficiently accurate. The main problem that comes up in the modelling of a VTM is to obtain accuracy of simulated results on all body segments in a certain range of air velocities, due to complex geometry of the human body and the combination of heat transfer processes between the body and its surroundings. In addition, it is very important that the numerical model can cover both natural and forced flow and that the body position can be easily adapted to different types of cabins. The aim of the research is to determine and investigate parameters of the numerical model that will give acceptable thermal behaviour of the VTM under both forced and natural convection. For validation purposes, the results from the simulations were compared with the published experimental results obtained using three physical manikins under different conditions.

The method

Numerical simulations were done in STAR CCM+ software. Mesh characteristics and turbulence models are identified as the most important factors in the process of the VTM development [6, 11, 16, 17]. In order to validate the numerical model of the virtual thermal manikin, relevant experimental data from measurements on physical thermal manikins must be considered, and three different experiments are chosen for this purpose.

– The experiments by Nilsson *et al.* on the thermal manikin "Comfortina" [14], based on the measurement of dry heat loss from the thermal manikin segments. The results of the measurement of air velocities and turbulence intensity behind the manikin are also published, making this experiment suitable for the verification of the numerical model in the initial set of simulation.
– The experiments by De Dear *et al*. on the thermal manikin "Monika" [12], where segmental heat transfer coefficients as well as their dependence on air velocity and airflow direction are determined. Horizontal airflow had velocities ranging from 0.2 to 5.0 m/s, including still air conditions.
– The experiment done on the thermal manikin made by P. T. Teknik [10]. The manikin was placed in a chamber with no forced airflow and segmental heat fluxes under natural convection conditions were determined.

All experiments were done in climate chambers, on manikins running with constant and uniform surface temperature. Different manikins, as well as the differences among the climate chambers and the conditions in these experiments, offer a range of data for the validation of the presented VTM.

The VTM geometry

The VTM should be applicable in a variety of vehicle cabin designs. Therefore, the VTM posture needs to be sufficiently adjustable, since there are differences in body postures in-

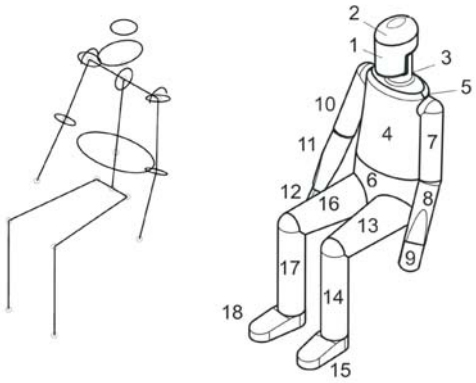

Figure 1. The VTM's skeleton and the VTM with numbered segments

side passenger vehicle cabins, commercial vehicles and agricultural tractors. For example, for the evaluation of thermal environment in passenger vehicles, the body is leaned backwards with the feet forward, in contrast to the upright sitting position in cabins of commercial vehicles.

The CAD model of the VTM body is a simplified humanoid in the sitting posture that, in this research, corresponds to the position in seats in commercial vehicle cabins. The manikin's body is symmetric, with its posture defined by characteristic points in places where the main body joints are (hips, shoulders, neck, elbows, *etc*.), fig. 1. In comparison with 3-D scanned manikins, there is an obvious benefit in CAD modelling of the simplified VTM geometry, since this makes it easily adjustable to different body postures and omits less important details. A similar approach is used in [6, 8, 18-21]. Main body dimensions are adopted from CATIA database for a 50th percentile European male, and the body is divided into 18 segments, fig. 1. The body surface area is compared to the areas of the chosen physical manikins in tab. 1.

Table 1. The VTM body surface area [m^2] in comparison with areas of physical manikins

VTM (male, sitting position)	Female manikin, "Comfortina", [14]	Female manikin, "Monika", [12]	Female manikin, [9]	Female manikin, P. T. Teknik, [11]
1.796	1.605	1.471	1.837	1.476

The numerical model

The initial parameters of the numerical model were based on published examples of numerical human body models as well as on the general recommendations for this type of problems in CFD [6, 10, 11, 16, 17]. The model was treated as a steady-state 3-D problem, with stationary bodies and boundaries. The flow was considered as turbulent incompressible flow. Heat exchange by thermal radiation was calculated using the diffuse grey surface-to-surface radiation model. The following parameters were varied in the initial set of simulations:

– surface mesh target size (size of the cells next to the VTM surface): 0.040, 0.035 or 0.030 m,
– the number of prism layers: 6, 8 or 12 layers, and
– turbulence model: RANS Realizable k-ε, RANS Standard k-ε or RANS SST k-ε.

All simulations were performed with the segregated (uncoupled) flow and energy model and with the two-layer approach that resolves the viscous sub-layer. The two-layer model is combined with both the high and the low y^+ wall treatment, as the most general one. The flow solver uses the SIMPLE algorithm, with the under-relaxation factor value of 0.7 for the velocity solver, and the under-relaxation factor value of 0.3 for the pressure solver. The variations of results that different settings produced were observed and evaluated taking into account the accuracy of the results, and convergence and the stability of residuals.

The mesh

The volume mesh consists of polyhedral finite volumes and near-wall orthogonal prismatic cell layers (called prism layers). The volume mesh is generated from the surface mesh, with local refinement on the VTM surface. The starting mesh size was the one with the largest finite elements (surface mesh size of 0.040 m) with six prism layers on the manikin's surface. This model has around 76,400 volume elements, with 10,424 surface elements on the VTM. The number of finite volumes is around 112,000 for the mesh with the surface elements of 0.035 m and around 143,000 for the mesh with the surface elements of 0.030 m in size. In the first case, the VTM surface is presented with 13,628 elements, and in the second case with 17,392 surface elements.

The VTM thermal characteristics

The problems with modelling the physiological response, moisture release and breathing are avoided by using the principle of equivalent temperature based on the dry heat loss from the body. The thermoregulation method of the VTM used in this research is the principle with the constant "skin" temperature. The VTM reacts to different thermal conditions by changes in the boundary heat flux, just like the physical manikins in the previously mentioned experiments. Therefore, the VTM surface was modelled as a solid wall with constant and uniform temperature of 34 °C, and surface emissivity was set to 0.95. The way the VTM is modelled allows for the implementation of other thermoregulation models, *e. g*. the constant heat flux model.

Boundary conditions

The boundary conditions in the initial set of the simulations were chosen according to the conditions in the experiment by Nilsson *et al*. [13, 14]. The chamber had the dimensions of 2.44 × 2.46 × 1.20 m ($L \times H \times W$), see fig. 4, left. The walls were modelled as no-slip walls with constant, uniform temperature of 21°C, and the evaluated value of wall emissivity was 0.9. Airflow with the temperature of $t_a = 20.4$ °C entered through the whole front area of the chamber, in front of the VTM. The boundary conditions at the inlet were the velocity of 0.27 m/s with mean turbulence intensity of 6% (experimental data, [14]). The air was evacuated through two circular openings on the back wall. In order to accelerate the analysis of the initial model settings, considering the domain longitudinally symmetric, the simulations were performed on the left half of the domain.

The setting of the initial case: results and discussion

The segmental heat fluxes were the most significant criterion for the comparison of different model settings with the experimental data, since they are in correlation with equivalent temperature. The total boundary sensible heat flux for a body segment Q_{seg} [Wm^{-2}] consists of convection C_{seg} [Wm^{-2}] and radiation heat flux R_{seg} [Wm^{-2}], eq. (1), and the same applies for the whole body. The boundary is the surface of a single VTM segment (scalp, head, neck, chest, *etc*.). The heat fluxes by convection and by radiation (C_{seg} and R_{seg} [Wm^{-2}], respectively), for one segment of the body can be calculated according to eq. (2) and eq. (3) [1]. In this case, the clothing area factor f_{cl} was equal to unity, because there was no clothing on the VTM. Consequently, clothes surface temperature t_{cl} was equal to skin temperature t_{sk}:

$$Q_{seg} = C_{seg} + R_{seg} \tag{1}$$

$$C_{\text{seg}} = f_{\text{cl}}\, h_{\text{Cseg}}(t_{\text{cl}} - t_{\text{a}}) \tag{2}$$

$$R_{\text{seg}} = f_{\text{cl}}\, h_{\text{Rseg}}(t_{\text{cl}} - t_{\text{mr}}) \tag{3}$$

Figure 2 shows the resulting boundary heat fluxes for different turbulence models. The highest discrepancy over the entire range of model settings is noted on the scalp (top of head). Looking at the values of segments and the whole body heat flux, RANS Realizable k-ε model of turbulence showed the best agreement with the experimental values, having 9% higher value of the boundary heat flux for the whole body. In addition, RANS Standard k-ε and RANS SST k-ω models had larger instability of the residuals. Decreasing the mesh size from 0.040 m to 0.035 m and 0.030 m had only a minor influence on the boundary heat flux, fig. 3. Changing the number of prism layers from six to eight decreased the difference between the whole body heat flux from the simulation and that from the experiment from 9% to 8%. Increasing the number of prism layers to 12, lead to the diverging solution residuals.

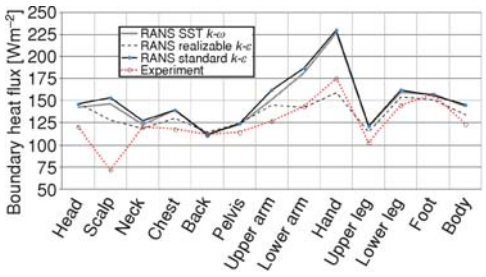

Figure 2. Segmental boundary heat fluxes for different turbulence models, in comparison with the experimental results

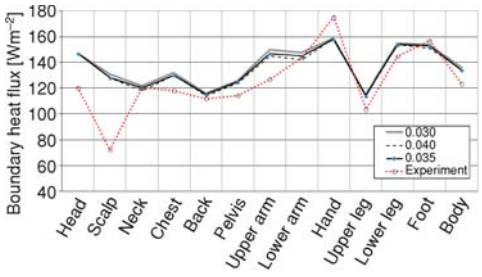

Figure 3. Segmental boundary heat fluxes for different mesh size, in comparison with the experimental results

The other criterion, the resulting air velocity profiles behind the VTM under different mesh settings, is shown in fig. 4. It can be seen that all the simulations gave profiles with the peak value at heights from 0.50 to 0.70 m. Since the air velocity profile behind the VTM is dependent on its shape, size and posture, it is expected to have different values in comparison to

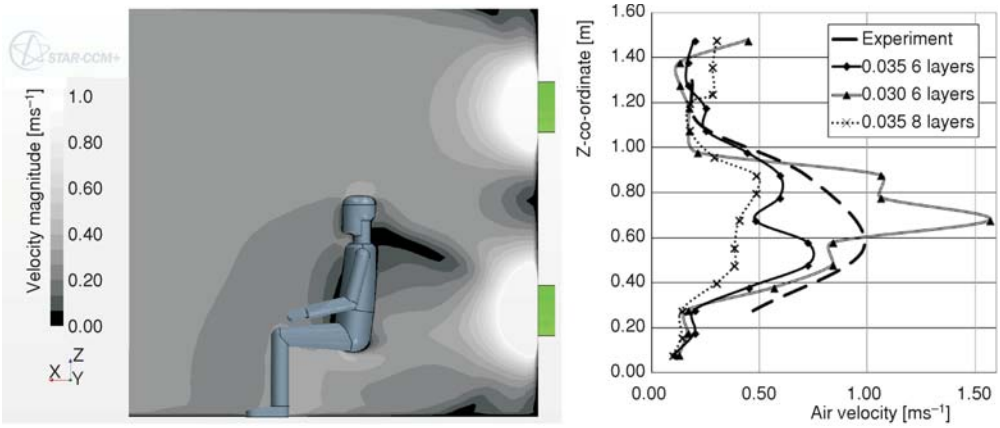

Figure 4. Left – The distribution of air velocity in the symmetry plane; right – air velocity profile behind the VTM for different mesh settings, in comparison with the experimental results

experimental data. Therefore, boundary heat fluxes and the stability of the solution were taken as a priority in determining the model settings. Consequently, the model with the mesh surface element of 0.035 m in size and with six prismatic boundary layers was chosen for further application. The maximum values of non-dimensional distance y^+ on the VTM surface were of the order of 5, which is in accordance with the results given in [11].

Finally, the simulation on the full model, *i. e.* with both left and right sides of the domain, showed acceptable agreement with both the experimental data and the results obtained with one half of the domain. Although the model and boundary conditions are theoretically symmetric, the simulation with both sides of the domain was necessary because of the turbulent nature of the flow and the presence of $v_y \neq 0$ in the symmetry plane.

The validation of the VTM

In order to validate the model under different forced flow conditions, the data from wind tunnel tests performed by de Dear *et al.* [12] were used. The parameters compared here were convective and radiative heat transfer coefficients. Since the airflow with uniform and unidirectional velocity profile could not be taken as a common condition inside vehicle cabins, and since there are local low velocities and natural convection flows present there, the VTM was tested under natural convection flow conditions too.

Convective heat transfer coefficients

Segmental convective heat transfer coefficients h_{Cseg} [$\mathrm{Wm^{-2}K^{-1}}$] were determined by excluding the radiation from the simulations, enabling the calculation of the convective heat transfer only. The virtual experiments were done with two air velocities (0.2 and 0.8 m/s) and under three azimuth angles (0, 45, and 90 degrees). The difference between VTM's surface temperature and chamber wall surface temperature was 12 °C.

Heat transfer coefficients for VTM segments h_{Cseg} and for the whole body h_{Cbody} were calculated according to:

$$h_{\mathrm{Cseg}} = \frac{C_{\mathrm{seg}}}{t_{\mathrm{sk}} - t_{\mathrm{a}}}, \qquad h_{\mathrm{Cbody}} = \frac{C_{\mathrm{body}}}{t_{\mathrm{sk}} - t_{\mathrm{a}}} \tag{4}$$

The calculated convective heat transfer coefficients were compared with the averaged regression values from the experimental measurements, fig. 5. It can be noted that the largest deviation is present in the head region (scalp, head, and neck), but other body parts show good agreement with the experimental data.

As far as the whole body convective heat transfer coefficients are concerned, larger deviation was present in the case with lower air velocity, despite a better distribution of the values over the segments. Local convective heat transfer coefficients obtained from the simula-

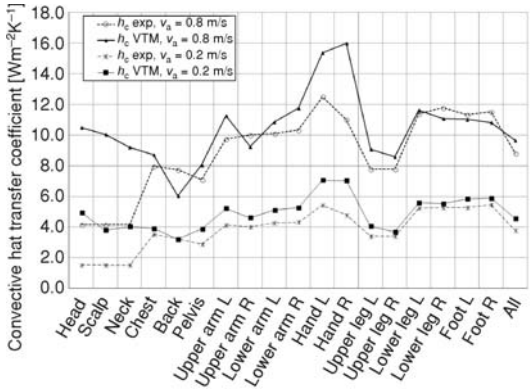

Figure 5. Convective heat transfer coefficients for body segments and for the whole body, averaged for all airflow directions, in comparison with the experimental results from [18]

tions were investigated more closely. Local maximum values of the heat transfer coefficients for head, scalp and neck, in the same case, were 38.6, 24.5, and 24.9 W/m^{2}K, respectively. These values indicate that there were no areas with an unrealistically high heat flux, which could have resulted from a deformed mesh, for example. The cause of the deviation in the head region was probably the presence of the physical manikin's shoulder-length hair, which increases the thermal insulation in the head region.

Linear radiative heat transfer coefficients

In this study, segmental linear radiative heat transfer coefficients $h_{R\text{seg}}$ [Wm^{-2}K^{-1}] were determined from radiative heat fluxes, eq. (5):

$$h_{R\text{seg}} = \frac{R_{\text{seg}}}{t_{\text{sk}} - t_{\text{mr}}} \tag{5}$$

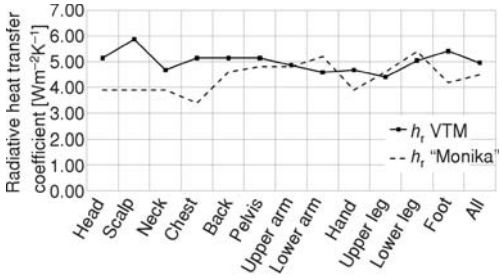

Figure 6. Linear radiative heat transfer coefficients for segments and for the whole body, in comparison with the experimental results from [18]

Mean radiant temperature obtained from the simulations was t_{mr} = 21.45 °C, whereas in De Dear's [12] experiment it was the same as the air and wall temperature: 18.85 °C. Due to the constant temperatures of the wall and the VTM surfaces, radiative heat flux was independent of air velocity and of the VTM orientation inside the chamber, with deviations within the limits of 1 W/m^2. Both the values of radiant heat transfer coefficients obtained by the simulation and the experimental values are shown in fig. 6. The linear radiative heat transfer coefficient for the whole body was 5.0 W/m^{2}K. This value is within the limits that can be found in the literature [1, 8], despite of a deviation in the upper body region.

Natural convection flow

In the virtual experiment with the natural convection flow, the VTM was placed in a 2.95 × 2.95 × 2.4 m chamber ($L \times W \times H$), with an air inlet at the bottom, and an outlet at the top of the chamber. Air velocity at the inlet was 0.02 m/s, with the temperature of 19.75 °C. The temperature of the VTM was uniform at 31°C, according to the conditions from the experiment described in [10].

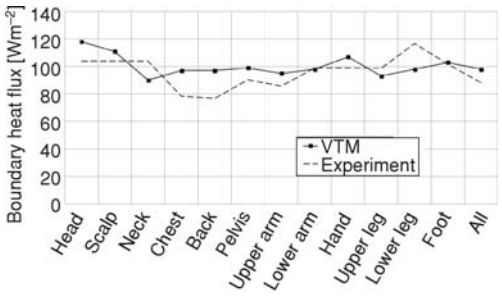

Figure 7. Total boundary heat flux in the case of natural convection flow for segments and for the whole body, in comparison with the experimental results from [10]

As it can be seen in fig. 7, the heat losses are close to those from the experimental data. Just like in previous cases, the largest deviations regarding convective heat transfer coefficients were present in the head region. The distribution of air velocity on the symmetry plane, shown in fig. 8, has a profile similar to the experimental results [10]. The average values of y^+ were between 0.5 and 2.5, which is higher

than the values given in [10]. This difference might be caused by the use of a different turbulence model (low Reynolds k-ε turbulence model was used in [10]), and/or by the fact that a smaller number of prismatic layers was used than in the model described in [10].

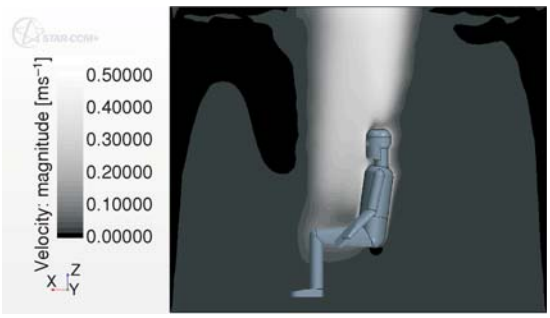

Figure 8. The distribution of air velocity on the symmetry plane in natural convection flow

Results and discussion

In comparison with other virtual thermal manikins mentioned in the Introduction [10, 11], the VTM with the mesh surface elements of 0.035 m in nominal size and with six layers of prismatic cells on the body surface, had a considerably coarser mesh, with around two to seven times smaller number of surface elements. The difference in the whole body heat flux between the experiment and simulation in the initial case was 9%, while the virtual manikin described in [11] had slightly better agreement (difference around 6%). The highest heat flux deviations were noted in the upper body region, but without unrealistically high values. For more complex flow situations that can be encountered in vehicle cabins, it is possible to increase the number of the VTM surface elements. Under the conditions used for validation, the difference was in the range of 2-5%.

The two-layer RANS Realizable k-ε turbulence model showed capability to cover forced as well as natural convection. Although pure natural convection is not a common occurrence in the investigation of thermal conditions inside vehicle cabins, the model must be able to cope with local conditions in the complex air velocity field around the VTM in the vehicle cabin, but there is no general rule for the choice of turbulence model. For example, for natural convection, other authors used low Reynolds number k-ε [9, 10], RNG k-ε [8, 19] or SST k-ω [6] turbulence model. Under forced airflow, Martinho *et al*. [11] concluded that the SST k-ω turbulence model showed the best matching with experimental results, while Kilic and Sevilgen [18] and Sevilgen and Kilic [20, 21] used RNG k-ε turbulence model for the investigation of thermal conditions in an automobile cabin with a virtual thermal manikin.

Conclusions

This paper presents a virtual model of the thermal manikin, which is meant to be used for thermal environment simulations in vehicle cabins. In contrast with the majority of similar numerical problems, where only one experiment is used for validation, the boundary heat fluxes, and heat transfer coefficients were compared with the published data from three experiments conducted on different thermal manikins. Several sets of virtual experiments covered a wider range of air velocities and airflow directions, from natural convection to uniform horizontal airflow with the velocity of up to 0.8 m/s.

The model with the mesh surface elements of 0.035 m in nominal size (around 13,600 surface elements) with six layers of prismatic cells on the body surface, and with the two-layer RANS Realizable k-ε turbulence, was chosen as a compromise between accuracy and computational time.

In general, the largest deviations can be noticed in the region of the head, but taking into account the differences between the shape of the VTM and those of real manikins or a hu-

man body, these results can be regarded as acceptable for comparative analysis. Larger discrepancies were noticed in the local thermal radiation heat transfer coefficients, although the overall value was within the limits that can be found in the literature.

This model is not directly applicable in the analyses of the latent heat loss from the VTM, contact with the seat or the presence of clothing. However, since the definition of the equivalent temperature is based on dry heat transfer, and since it can be determined with the use of an unclothed manikin, any further work will primarily be focused on the use of the VTM for the optimization of the cabin ventilation system.

Acknowledgments

This research was done as a part of the project TR35041 – Investigation of the safety of the vehicle as part of cybernetic system: Driver-Vehicle-Environment, which was supported by the Serbian Ministry of Education, Science and Technological Development of the Republic of Serbia. The authors wish to thank Dr. Maša Bukurov for enabling the use of the licensed CFD software.

Nomenclature

C – convective heat flux, [Wm^{-2}]
f_{cl} – clothing area factor, [–]
h_C – convective heat transfer coefficient, [$Wm^{-2}K^{-1}$]
h_R – linear radiative heat transfer coefficient, [$Wm^{-2}K^{-1}$]
Q – total heat flux through the body surface, [Wm^{-2}]
R – radiative heat flux, [Wm^{-2}]
t_a – air temperature, [°C]
t_{cl} – clothes surface temperature, [°C]
t_{mr} – mean radiant temperature, [°C]
t_{sk} – skin temperature, [°C]

Subscripts

body – whole body
seg – segmental

References

[1] Parsons, K., *Human Thermal Environments: The Effects of Hot, Moderate and Cold Environments on Human Health, Comfort and Performance*, 2nd ed., Taylor & Francis, London, UK, 2003
[2] Nilsson, H., Comfort Climate Evaluation with Thermal Manikin Methods and Computer Simulation Person, Ph. D. thesis, University of Gavle, Gavle, Sweden, 2004
[3] ***, ISO 14505-2, Ergonomics of the Thermal Environment – Evaluation of the Thermal Environment in Vehicles, Part 2: Determination of Equivalent Temperature, 2008
[4] Han, T., *et al*., Virtual Thermal Comfort Engineering, SAE paper 2001-01-0588, 2001
[5] Huizenga, C. *et al*., A Model of Human Physiology and Comfort for Assessing Complex Thermal Environments, *Building and Environment, 36* (2001), 6, pp. 691-699
[6] Voelker, C., Kornadt, O., Human Body's Micro-Climate: Measurement and Simulation for the Coupling of CFD with a Human Thermoregulation Model, *Proceedings*, Building Simulation, 12th Conference of International Building Performance Simulation Association, Sydney, Australia, 2011, pp. 2048-2054
[7] Tanabe, S., *et al.*, Evaluation of Thermal Comfort Using Combined Multi-Node Thermoregulation (65MN) and Radiation Models and Computational Fluid Dynamics (CFD), *Energy and Buildings, 34* (2002), 5, pp. 637-646
[8] Kilic, M., Sevilgen, G., Modelling Airflow, Heat Transfer and Moisture Transport Around a Standing Human Body by Computational Fluid Dynamics, *International Communications in Heat and Mass Transfer, 35* (2008), 9, pp. 1159-1164
[9] Zhu, S., *et al*., Development of a Computational Thermal Manikin Applicable in Non-Uniform Thermal Environment – Part 2: Coupled Simulation Using Sakoi's Human Thermal Physiological Model, *HVAC&R Research, 14* (2008), 4, pp. 545-564

[10] Sorensen, D. N., Voigt, L. K., Modelling Flow and Heat Transfer around a Seated Human Body by Computational Fluid Dynamics, *Building and Environment, 38* (2003), 6, pp. 753-762
[11] Martinho, N., *et al*., CFD Modelling of Benchmark Tests for Flow around a Detailed Computer Simulated Person, *Proceedings*, 7th International Thermal Manikin and Modelling Meeting, University of Coimbra, Portugal, 2008
[12] De Dear, R., *et al*., Convective and Radiative Heat Transfer Coefficients for Individual Human Body Segments, *International Journal of Biometeorology, 40* (1997), 3, pp. 141-156
[13] Nilsson, H., *et al.*, CFD Modeling of Thermal Manikin Heat Loss in a Comfort Evaluation Benchmark Test, *Proceedings*, Roomvent 2007, 10th International Conference on Air Distribution in Buildings, Helsinki, Finland, 2007
[14] Nilsson, H., *et al*., Benchmark Test for a Computer Simulated Person – Manikin Heat Loss for Thermal Comfort Evaluation, Aalborg University, Denmark, and Gavle University, Sweden, 2007
[15] Ružić, D., Analysis of Airflow Direction on Heat Loss from Operator's Body in an Agricultural Tractor Cab, *Proceedings* (Ed. S. Košutić), 40th International Symposium Actual Tasks on Agricultural Engineering, 2012, Opatija, Croatia, pp. 161-169
[16] Ferziger, J. H., Perić, M., *Computational Methods for Fluid Dynamics*, 3rd ed., Springer Verlag, Berlin, Germany, 2002
[17] ***, STAR-CCM+, User Guide, CD-Adapco, 2011
[18] Kilic, M., Sevilgen, G., Evaluation of Heat Transfer Characteristics in an Automobile Cabin with a Virtual Manikin during Heating Period, *Numerical Heat Transfer, Part A: Applications, 56* (2009), 6, pp. 515-539
[19] Sevilgen, G., Kilic, M., Numerical Analysis of Air Flow, Heat Transfer, Moisture Transport and Thermal Comfort in a Room Heated by Two-Panel Radiators, *Energy and Buildings, 43* (2011), 1, pp. 137-146
[20] Sevilgen, G., Kilic, M., Three Dimensional Numerical Analysis of Temperature Distribution in an Automobile Cabin, *Thermal Science, 16* (2012) 1, pp. 321-326
[21] Sevilgen, G., Kilic, M., Investigation of Transient Cooling of an Automobile Cabin with a Virtual Manikin Under Solar Radiation, *Thermal Science, 17* (2013), 2, pp. 397-406

Paper submitted: January 15, 2013
Paper revised: July 26, 2013
Paper accepted: August 5, 2013